SANYO DENKI Technical Report No.5 May 1998

General Theses

Self-Compensating Control for Suppression of Rotational Speed Variation Generated in a Geared Servo System

Masahiko Itoh

1. Introduction

The merit of using gear reducers in servo-controlled mechanical systems is that the power transfer system can be designed in a compact configuration with high efficiency by using a higher motor rotation speed in comparison with a direct-drive motor. In practice, however, when a reducer is installed in a mechanical system, the required dynamic characteristics of the system may not be achieved due to velocity and torque ripples in the lower frequency range of the bandwidth of the main control system even though the adequate selection is made in accordance with the specifications. Because, velocity and torque ripples occur inside the gear reducer depending upon its structure and the rotational speed of the input shaft, and excite the driven machine system.
To overcome this problem, a gear reducer with self-compensating control function is proposed and its fundamental performance is described in the previous Technical Report (1). In summary, the excitation components that occur in the lower frequency range caused by the structure of the reducer itself, are detected by a pulse generator attached to the final geared stage without reducing the torsional stiffness of the reducer. The ripple component detected by the pulse generator is fed back to the servo amplifier for compensation.
This report clarifies the effectiveness of this technique by investigating the stability, the command following performance and the disturbance rejection performance of the control system, assuming that the self-compensating control is applied to a mechanical system. In addition, this report describes the suppression effect on the rotational speed variations which occur at passing through resonance in the mechanical system composed of the harmonic drive gear reducer [(2) (3)].

2. Internal Exciting Torque Generated inside the Gear Reducer

The equation of motion, which describes the torsional vibration of the mechanical system including the gear reducer, can be expressed by the differential equation assuming that the stiffness of the gearing is constant.

$$M\ddot{X}+C\dot{X}+KX=T_{rq} \text{---(1)}$$

where $\boldsymbol{M}$, $\boldsymbol{C}$, and $\boldsymbol{K}$ represent a mass matrix, a damping matrix and a stiffness matrix, respectively. In addition, $\boldsymbol{Trq}$ represents an external exciting torque vector and $\boldsymbol{X}$ indicates a displacement vector. If an angle transmission error $\boldsymbol{e}(t)$ (error vector) exists at the geared stage, Eq.(1) is rewritten as

$$M\ddot{X}+C\dot{X}+K(X-e)=T_{rq} \text{---(2)}$$

Further, when M is not singular, Eq.(2) is expressed as

$$\left.\begin{aligned} \ddot{X} &= M^{-1}(-C\dot{X}-KX+T_{rg}+Q_d) \\ Q_d &= K\,e \end{aligned}\right\} \text{---(3)}$$

Consequently, an internal exciting torque Q_d (vector) is locally generated inside the gear reducer.
A typical example of such internal excitation can be found in the harmonic drive gear system. Fig. 1 shows a schematic diagram of the gear head [2][3] with a sensor for self-compensating control using the harmonic drive gear reducer. Various researches have been investigated the causes of the internal excitation [4] to [7]. Here, the cause of the internal excitation locally generated inside the harmonic drive gear system is assumed from the study of Hidaka [4] et al. to be the angle transmission error that is produced by the radial alignment errors at the circular spline and flexspline. Denoting the variable component of the angle transmission errors between the input and the output shafts as θ_e,

$$\theta_e = \frac{\tan\alpha}{r_c}\left[\sum_{i=2}^{\infty} A_{ci}\sin(i\theta_c+\psi_{ci}) + \sum_{i=2}^{\infty} A_{fi}\sin(i\theta_f+\psi_{fi})\right] \text{---(4)}$$
$$(i=2, 4, 6\cdots)$$

$$\theta_c = \int \omega_m(t)\,dt, \quad \theta_f = \int (Z_c/Z_f)\,\omega_m(t)\,dt \text{---(5)}$$

where,

α	: pressure angle of teeth
r_c	: pitch radius of the circular spline
Z_c, Z_f	: number of teeth of the circular spline and the flexspline, respectively
A_{ci}, A_{fi}	: i-th amplitude (radial direction error)
ψ_{ci}, ψ_{fi}	: i-th phase angle

Eq. (3) shows that an internal exciting torque that is generated inside the gear reducer, can be expressed by the product of the variable component θ_e of the angle transformation error and torsional stiffness K_g of the reducer. Consequently the variable component $Q_d(t)$ of the torque (scalar) is expressed as

$$\begin{aligned} Q_d(t) &= K_g\theta_e \\ &= K_g\left[\frac{\tan\alpha}{r_c}\left\{\sum_{i=2}^{\infty} A_{ci}\sin(i\theta_c+\psi_{ci}) + \sum_{i=2}^{\infty} A_{fi}\sin(i\theta_f+\psi_{fi})\right\}\right] \text{---(6)} \\ &\quad (i=2, 4, 6\cdots) \end{aligned}$$

Eq. (6) shows that $Q_d(t)$ consists of the fundamental component of two cycles per motor revolution and its higher harmonics. In this case, each variation component has a beat frequency, since Z_c is nearly equal to Z_f.

3. Variable Self-Compensating Control

Fig. 2 shows the block diagram of the geared motor system composed of the self-compensating type gear head with the self-compensating control loop that consists of variable center frequency type tracking band-pass filters, and the driven machine system.

ω_{cmd} : velocity command

ω_m : rotating speed of the motor (= rotating speed of the wave generator)
ω_g : rotating speed of the gear reducer's output shaft
ω_l : rotating speed of the driven machine
θ_m : angular rotation of the motor
θ_g : angular rotation of the gear reducer's output shaft
θ_l : angular rotation of the driven machine
R_g : reduction ratio of the gear reducer
i : current of the armature
R : motor armature resistance
L : motor armature inductance
K_t : torque constant
K_e : voltage constant
K_c : current loop gain
K_{cb} : current feedback gain
K_v : proportional gain of the PI control in the velocity control system
T_i : integral time constant of the PI control in the velocity control system
J_m : moment of inertia of the motor
J_g : moment of inertia of the reducer's output shaft
J_l : moment of inertia of the driven machine
K_g : torsional stiffness of the reducer
K_s : torsional stiffness between the reducer's output shaft and the driven machine
C_g : damping factor of the reducer
C_s : damping factor between the reducer's output shaft and the driven machine

$G_v(s)$ represents the transfer function of the PI control in the velocity control system.

$$G_v(s) = K_v(1 + 1/T_i s) \quad \text{---(7)}$$

$G_b(s)$ shows the transfer function of the self-compensating control loop, which is composed of three band-pass filters and feedback gains in parallel, in order to reduce up to the third component of variations (cf., Eq. 6) generated within the bandwidth of the main control loop. Following up the velocity command value, the center frequencies of band-pass filters ω_{oi} (i = 1 ~ 3) are set to twice, four times and six times of the motor rotating frequency as

$$\left.\begin{aligned} \omega_{o1}(t) &= 4\pi N_m(t)/60 \\ \omega_{o2}(t) &= 2\omega_{o1}(t) \\ \omega_{o3}(t) &= 3\omega_{o1}(t) \end{aligned}\right\} \quad \text{---(8)}$$

The center frequencies of tracking band-pass filters ω_{oi} (i = 1 ~ 3) are time-varying, while Q factors of the band-pass filters are constant (Q_{oi} = const.). The state equation that indicates the performance of the system composed of the driven mechanical system and the driving system (electrical and mechanical systems), is as follows.

$$dx/dt = Ax + Bu + Eq \quad \text{---(9)}$$
$$y = Cx \quad \text{---(10)}$$

u, q, x and y represent an input variable, a disturbance, a state vector and an output vector, respectively, where $u = \omega_{cmd}$ and $q = Q_d(t)$. As α_j and β_j (j = 1 ~ 3) are the state variables of the band-pass filters, and K_{bj} (j = 1 ~ 3) is the feedback gain of

the self-compensating control loop, and each vector and the coefficient matrixes are expressed as follows:

$$\boldsymbol{x}=[i\ \ \theta_m\ \omega_m\ \theta_g\ \omega_g\ \theta_l\ \omega_l\ \eta\ \alpha_1\ \beta_1\ \alpha_2\ \beta_2\ \alpha_3\ \beta_3]^T,$$

$$\boldsymbol{y}=[\omega_m\ \omega_g]^T,$$

$$\boldsymbol{B}=[K_cK_v/L\ \ 0\ 0\ 0\ 0\ 0\ 0\ 1\ 0\ 0\ 0\ 0\ 0\ 0]^T,$$

$$\boldsymbol{C}=\begin{bmatrix}0&0&1&0&0&0&0&0&0&0&0&0&0&0\\0&0&0&0&1&0&0&0&0&0&0&0&0&0\end{bmatrix},$$

$$\boldsymbol{E}=[0\ \ 0\ \ -1/J_mR_g\ \ 0\ \ 1/J_g\ \ 0\ 0\ 0\ 0\ 0\ 0\ 0\ 0\ 0]^T,$$

$$\boldsymbol{A}=\begin{bmatrix}\boldsymbol{A}_{11}&\boldsymbol{A}_{12}\\\boldsymbol{A}_{21}&\boldsymbol{A}_{22}\end{bmatrix}$$

where,

$$\boldsymbol{A}_{11}=\begin{bmatrix}-\frac{K_cK_b+R}{L}&0&-\frac{K_c+K_cK_v}{L}&0&0&0&0&\frac{K_cK_v}{LT_i}\\0&0&1&0&0&0&0&0\\\frac{K_t}{J_m}&-\frac{K_g}{J_mR_g^2}&-\frac{C_g}{J_mR_g^2}&\frac{K_g}{J_mR_g}&\frac{C_g}{J_mR_g}&0&0&0\\0&0&0&0&1&0&0&0\\0&\frac{K_g}{J_gR_g}&\frac{C_g}{J_gR_g}&-\frac{K_g+K_t}{J_g}&-\frac{C_g+C_t}{J_g}&\frac{K_t}{J_g}&\frac{C_t}{J_g}&0\\0&0&0&0&0&0&1&0\\0&0&0&\frac{K_t}{J_l}&\frac{C_t}{J_l}&-\frac{K_t}{J_l}&-\frac{C_t}{J_l}&0\\0&0&-1&0&0&0&0&0\end{bmatrix},$$

$$\boldsymbol{A}_{12}=\begin{bmatrix}0&-\frac{K_{b1}K_c\omega_{e1}(t)}{LQ_{e1}}&0&-\frac{K_{b2}K_c\omega_{e2}(t)}{LQ_{e2}}&0&-\frac{K_{b3}K_c\omega_{e3}(t)}{LQ_{e3}}\\\multicolumn{6}{c}{\boldsymbol{0}_{6\times7}}\end{bmatrix},$$

$$\boldsymbol{A}_{21}=\begin{bmatrix}0&0&0&0&0&0&0&0\\0&0&0&0&1&0&0&0\\0&0&0&0&0&0&0&0\\0&0&0&0&1&0&0&0\\0&0&0&0&0&0&0&0\\0&0&0&0&1&0&0&0\end{bmatrix},$$

$$\boldsymbol{A}_{22}=\begin{bmatrix}0&1&0&0&0&0\\-\omega_{e1}^2(t)&-\frac{\omega_{e1}(t)}{Q_{e1}}&0&0&0&0\\0&0&0&1&0&0\\0&0&-\omega_{e2}^2(t)&-\frac{\omega_{e2}(t)}{Q_{e2}}&0&0\\0&0&0&0&0&1\\0&0&0&0&-\omega_{e3}^2(t)&-\frac{\omega_{e3}(t)}{Q_{e3}}\end{bmatrix}$$

, and η is defined as

$$\eta\equiv\int(\omega_{cmd}-\omega_m)\,dt \quad \text{---(11)}$$

4. Characteristics of Self-Compensating Control System

4.1 Stability

When the center frequencies of the tracking band-pass filters change with the change of motor rotation speed, the system stability is considered by calculating the loci of system eigenvalues, assuming that the system matrix $\boldsymbol{A}$ changes slowly with the changes of the center frequencies. Table 1 shows the parameter values that are used for simulations. Fig. 3 shows the loci of system eigenvalues around the imaginary axis when the conditions of the feedback gain $\boldsymbol{K}_{b\,3}$ of the self-compensating control loop are changed. When $\boldsymbol{K}_{b\,3} = 120$ where the feedback gain for the higher-order ripple component has a high gain, the system becomes unstable as the motor axis rotating speed exceeds 2158 min^{-1} ($\omega_{o1} = 452$ rad/sec). Therefore, when $\boldsymbol{K}_{b\,3}$ is set at around 120 in order to decrease the higher harmonic component $6\boldsymbol{N}_{\text{m}}$ in the lower motor speed range, $\boldsymbol{K}_{b\,3}$ must be lowered in a higher motor speed range to satisfy the stability conditions of the system.
Consequently, considering the stability conditions and compensation effects within the bandwidth which is the objective of this method, $\boldsymbol{K}_{b\,3}$ is set to zero and the third variation component is not fed back into the current loop in the higher motor speed range.

Table 1 Simulation conditions

Parameter		Value	Unit
Moment of inertia	J_m	1.011×10^{-5}	kg·m2
	J_g	6.565×10^{-5}	
	J_l	8.205×10^{-4}	
Torsional stiffness	K_g	5053.5	N·m/rad
	K_s	80.984	
Damping coefficient	C_g	0.13	N·m·sec/rad
	C_s	0.013	
Gear reducer			
Reduction ratio	R_g	50.0	-
Pressure angle	α	30.0	degree
Pitch diameter	$2r_c$	38.0	mm
Number of teeth	Z_c,Z_f	204,200	-
Radial error	A_{c2},A_{f2}	3.0,2.0	μm
	A_{c4},Af4	5.5,5.0	
	A_{c6},A_{f6}		
	3.0,2.0		
ψ_{ci},ψ_{fi} (i = 2,4,6)	0.0,0.0	degree	
Velocity loop gain	K_v	0.3913	A/(rad/sec)
Integral time constant	T_i	0.00563	sec
Torque constant	K_t	0.2633	N·m/A
Voltage constant	K_e	0.1810	V/(rad/sec)
Phase resistance	R	35.0	Ω
Phase inductance	L	0.022	H
Current loop gain	K_c	3.05	V/A
Current feedback gain	K_{cb}	1.0	-
Self-compensating loop feedback gain	K_{b1}	30.0	A/(rad/sec)
	K_{b2}	60.0	
	K_{b3}	120.0	; if Nm≦1800min^{-1}
		0.0	; else if Nm≧1800min^{-1}
Q factor of band-pass filter	Q_{o1}	12.0	-
	Q_{o2}	20.0	
	Q_{o3}	25.0	

4.2 Command Following Performance

Setting $\boldsymbol{q} = 0$, the transfer function matrix $\boldsymbol{G}u(s)$, which represents the command following performance between the velocity command ω_{cmd} and the rotating speed, is obtained from Eq.(9) and (10) as

$$\boldsymbol{G}_u(s) = [G_{u11}\ G_{u12}]^T = \boldsymbol{C}(s\boldsymbol{I} - \boldsymbol{A})^{-1}\boldsymbol{B} \quad \text{---(12)}$$

The transfer function ω_g / ω_{cmd} for the reducer's rotation speed of velocity command ωcmd is the $\boldsymbol{G}u12\ (s)$ component of $\boldsymbol{G}u\ (s)$. Command following performance is investigated when the loading inertia is directly connected to the reducer's output shaft. The mechanical parameters of the driven machine part are as follows:

$J_l = 2.539 \times 10^{-4}\ \mathrm{kg \cdot m^2}$

$K_s = 16000.0\ \mathrm{N \cdot m/rad}$

$C_s = 0.13\ \mathrm{N \cdot m \cdot sec/rad}$

The other simulation parameters are given in Table 1. Fig. 4 shows the bode plots (result of simulation) of the transfer function ω_g / ω_{cmd} using the self-compensating control loop set to the motor speed of 750 $\mathrm{min^{-1}}$. The reverse triangle mark (▽) in Fig. 4 represents the internal exciting frequencies (25, 50 and 75 Hz).
In Fig. 4, a peak of about 580 Hz noted by the black reverse triangle mark (▼) represents the first natural frequency of the torsional vibration of the mechanical system. This figure shows that $\boldsymbol{G}u12\ (s)$ has band-eliminating characteristics due to the band-pass filters of the self-compensating control loop.

4.3 Disturbance Rejection Performance

Setting $\boldsymbol{u} = 0$, the transfer function matrix $\boldsymbol{G}d\ (s)$, which represents the disturbance rejection performance of the self-compensating control loop, is obtained from Eq.(9) and (10) as

$$\boldsymbol{G}_d(s) = [G_{d11}\ G_{d12}]^T = \boldsymbol{C}(s\boldsymbol{I} - \boldsymbol{A})^{-1}\boldsymbol{E} \quad \text{---(13)}$$

The transfer function $\omega_g / \boldsymbol{Q}d$ for the reducer's rotation speed of the internal excitation $\boldsymbol{Q}d$ is the $\boldsymbol{G}u12\ (s\ )$ component of $\boldsymbol{G}d\ (s)$.
Fig. 5 shows the bode plots of the transfer function $\omega_g / \boldsymbol{Q}d$ when the self-compensating control loop set for the motor speed of 750 $\mathrm{min^{-1}}$ is used. This figure shows that the self-compensating control suppresses the speed variations of the reducer generated by the internal exciting components (at 25, 50 and 75 Hz noted by the reverse triangle (▽) in Fig. 5) which occur depending upon the rotating speed.

5. Simulation on Suppression of Vibration when Passing Through Resonance

Vibration suppression effects when passing through resonance are examined by simulation. Table 1 shows the values of parameters used for the simulations. Values of the radial direction errors ($\boldsymbol{A}ci$, $\boldsymbol{A}fi$, Ψci, Ψfi : $i = 2, 4, 6$) of the harmonic drive gear reducer are set referring to the reference (4). The first natural frequency of the torsional vibration of the mechanical system is 50 Hz. In this simulation, the time historical response of the rotating speed ω_l of the driven mechanical system is calculated by the Runge-Kutta method. To avoid excitation of the free vibration in

the driven machine system, the angular acceleration is set to 62.8 rad/sec^2 (converted to motor shaft). This condition means that the motor rotation speed is accelerated or reduced to 3000 min^{-1} in five seconds. On the other hand, ***Kb3*** will be set to zero on the condition of $Nm \cong 1800$ min^{-1} of the motor speed to satisfy the stability condition.
Fig. 6 shows simulation results. This figure shows that the applied variable self-compensating control suppresses the vibration level of the loading inertia when passing through resonance (Nm = 500, 750 and 1500 min^{-1} of the motor speed) by reducing the excitation components locally generated inside the gear reducer.

6. Experimental Results and Considerations

6.1 Hardware Configuration

Fig. 7 shows a configuration of the geared motor system with the variable self-compensating control system that is configured to reduce velocity ripple generated by internal exciting torque shown by Eq. (6). To detect the velocity ripples that are locally generated inside the gear reducer, a magnetic pulse encoder with 1000 pulses/rev. is equipped with a final geared stage without decreasing the torsional stiffness of the output shaft. The output pulses are converted to an analog signal through the F/V converter with a frequency doubler, and the variable component to be decreased is fed back to the current input of the servo amplifier through band-pass filters.
The tracking band-pass filters that are integrated into the self-compensating control loop are composed of switched capacitor filters. Their center frequencies keep tracking the velocity command generated from the pulse generator and are adjusted to the speed variation components locally generated at the final geared stage. The velocity variation components that are fed back to the current loop of the servo amplifier are limited to the third-order component considering the stability and expecting compensation effects within the bandwidth of the main control loop. In addition, taking the simulation results of sections 4.1 and 5 into account, the feedback gain Kb3 is set to zero by the gain selector and is not fed back to the current loop to stabilize the system when the motor speed $Nm \cong 1800$ min^{-1}.

6.2 Suppression Effects on the Rotational Speed Variations under No-loading

Fig. 8 shows effects of the self-compensating control under no-loading at the steady-state motor rotation. The horizontal axis represents the frequency and the vertical axis indicates the velocity ripple at each motor speed. This figure shows that variation components of $2Nm$, $4Nm$ and $6Nm$ are reduced down to 1/3 ~ 1/2.

6.3 In the Case of Loading Condition

Fig. 9 outlines the experimental set-up with loading inertia. The velocity signal of the loading inertia is detected with an encoder of 81,000 pulses/revolution and it is analyzed after being converted to an analog signal through the F/V converter. The physical parameters of this experimental set-up are shown in Table 2. The first natural frequency of the torsional vibration of the loading mechanical system is 50 Hz.
Fig. 10 shows suppression effects on the vibration level of the loading inertia at the steady-state motor speed. At the motor speeds of 500, 750, and 1500 min^{-1} where the variation components of $6Nm$, $4Nm$ and $2Nm$ resonate at the natural frequency, the speed variation level of the loading inertia is increased. The variable self-compensating control applied to the harmonic drive gear reducer clearly

suppresses the vibration level down to 1/3 to 1/2.

Table 2 Physical parameters of the experimental set-up

Parameter		Value	Unit
Moment of inertia	J_m	1.011×10^{-5}	kg·m2
	J_g	6.565×10^{-5}	
	J_l	8.205×10^{-4}	
Torsional stiffness	K_g	5053.5	N·m/rad
	K_s	80.984	
Damping coefficient	C_g	0.13,	N·m·sec/rad
	C_s	0.013	
Reduction ratio of gear reducer	R_g	50.0	-

6.4 Suppression Effects when Passing Through Resonance

Fig. 11 shows suppression effects of vibration when passing through resonance. The condition of angular acceleration is 62.8 rad/sec^2 (converted to motor shaft). Fig. 11 shows the suppression effect of about 1/3 ~ 1/2 to the uncompensated vibration level in this case, too.

7. Conclusion

A variable self-compensating control technique to reduce the speed variation locally generated inside the gear reducer, is applied to the harmonic drive gear reducer. Its fundamental characteristics and installation effects in the servo system were examined theoretically and experimentally. The results of this report are summarized below.

(1) The effects of this self-compensating control system were clarified by simulating the stability, command following characteristics and disturbance rejection performance.

(2) Using the self-compensating control loop, the variation of no-loading inertia can be suppressed down to about 1/3 ~ 1/2. (3) From the simulations and experiments on the system of the loading inertia, it was confirmed that the self-compensating control system can suppress vibration when passing through resonance. The simulation results agreed well with the experiment results qualitatively. The velocity variation can be suppressed down to about 1/3 ~ 1/2.

References

(1) Itoh, M., 1996-5, "Basic Study on the Gear Reducer with Self-compensating Control," SANYO DENKI Technical Report, No.1, pp.43-48.

(2) Itoh, M. et al., 1996, "Suppression of Rotational Speed Variation Excited by Reduction Gear Mechanism by Means of Self-Compensating Control (1st Report: Reduction of Exciting Components of Harmonic Drive Gear)," Trans.

Jpn. Soc. Mech. Eng., (in Japanese), Vol.62, No.595(C), pp.860-867.

(3) Itoh, M. et al., 1996, "Suppression of Rotational Speed Variation Excited by Reduction Gear Mechanism by Means of Self-Compensating Control (2nd Report: Effects of Tracking Band-Pass Filters Integrated into Self-Compensating Control Loop)," Trans. Jpn. Soc. Mech. Eng., (in Japanese), Vol.62, No.604(C), pp.4551-4557.

(4) Hidaka, T. et al., 1989, "Theoretical Analysis of the Vibration in a Robot due to a Strain Wave Gearing," Trans. Jpn. Soc. Mech. Eng., (in Japanese), Vol.55, No.516(C), pp.1864-1871.

(5) Yanabe, S. et al., 1989, "Torsional Stiffness of Harmonic Drive Reducers," Trans. Jpn. Soc. Mech. Eng., (in Japanese), Vol.55, No.509(C), pp.216-221.

(6) Yanabe, S. et al., 1990, "Rotational Transmission Error of Harmonic Drive Device," Trans. Jpn. Soc. Mech. Eng., (in Japanese), Vol.56, No.521(C), pp.148-153.

(7) Hidaka, T. et al., 1986, "Torsional Vibration in the Robot Due to Wave Gears," Trans. Jpn. Soc. Mech. Eng., (in Japanese), Vol.52, No.480(C), pp.2207-2212.

Masahiko Itoh
Joined company in 1988
Technology Development Division
Worked on study and development of motion and vibration control
Dr. Eng.

Fig.1 Schematic diagram of a gear head with a sensor for self-compensating control

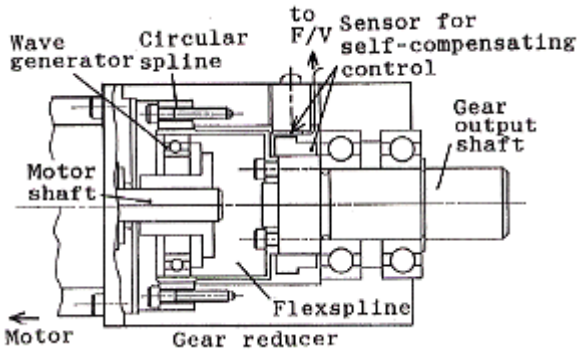

Fig.2 Block diagram of the geared motor system with the variable self-compensating control loop

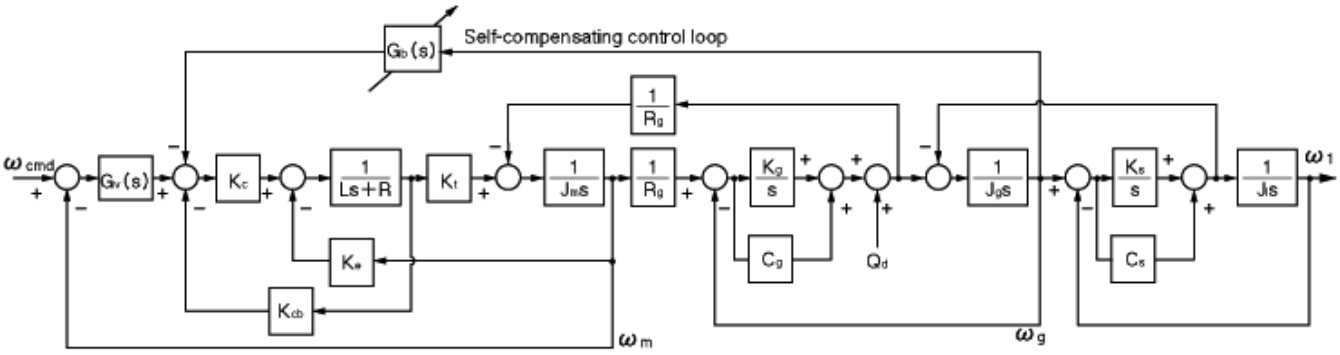

Fig.3 Loci of system eigenvalues

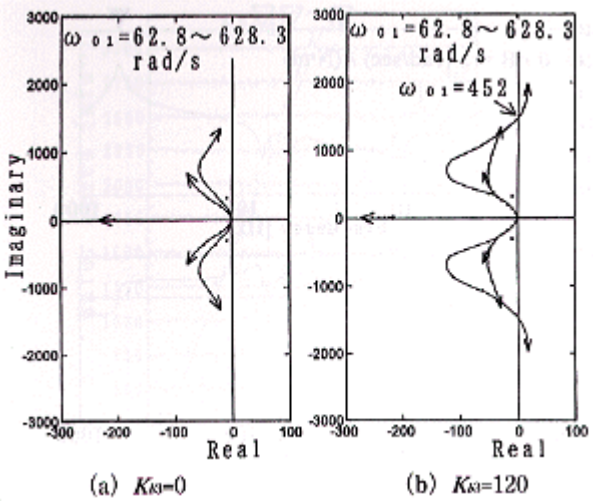

(a) $K_{\omega 3}$=0　　(b) $K_{\omega 3}$=120

Fig. 4 Bode plots of ω_g/ω_{cmd}

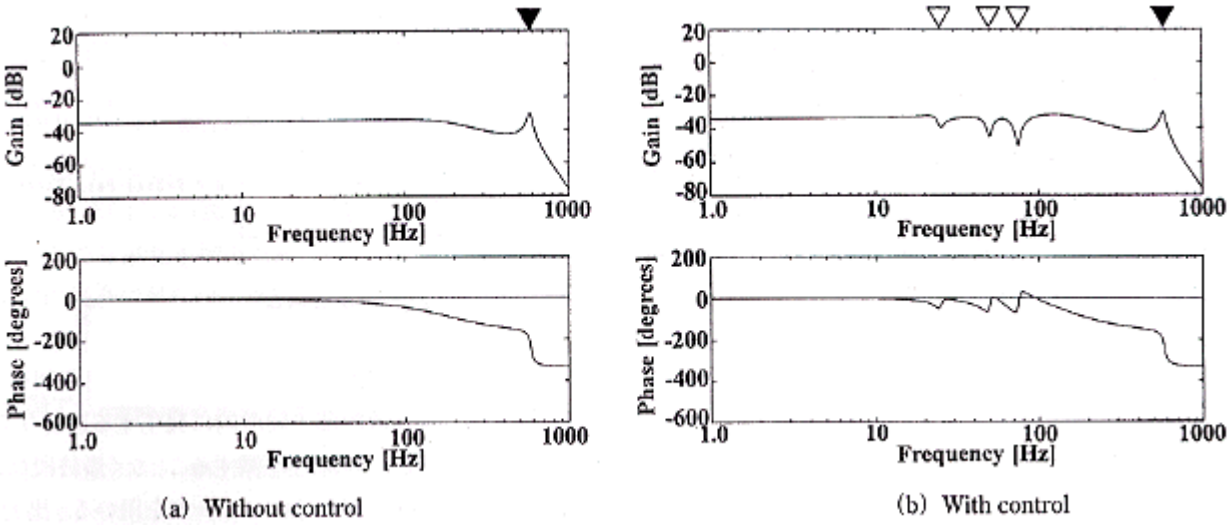

(a) Without control

(b) With control

Fig.5 Bode plots of ω_g/Q_d

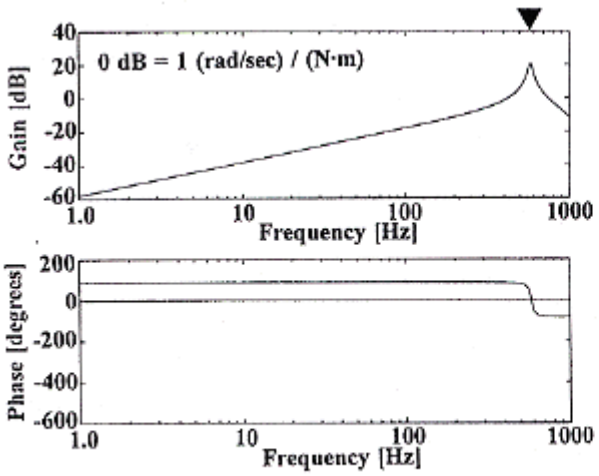

(a) Without control

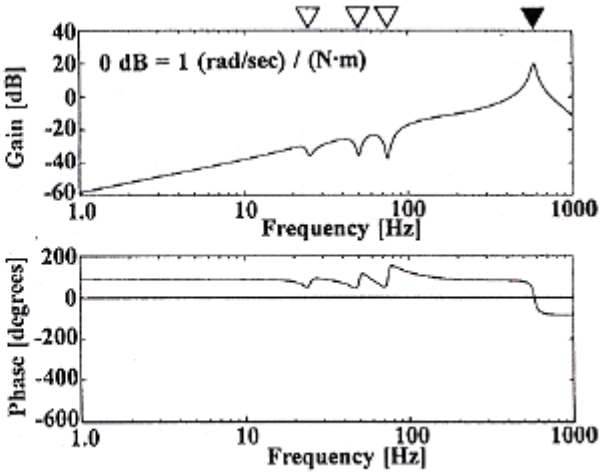

(b) With control

Fig.6 Suppression effects when passing through resonance (simulation)

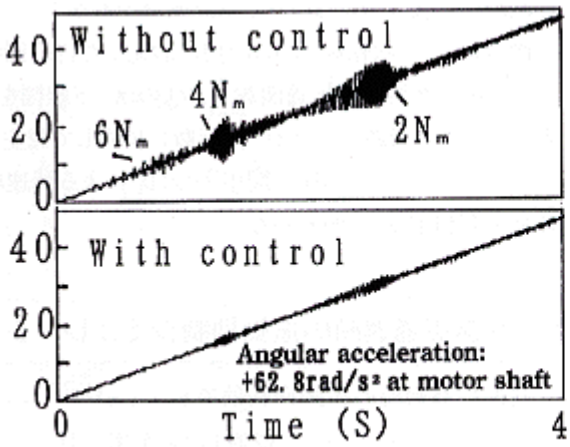

(a) Increasing the motor speed

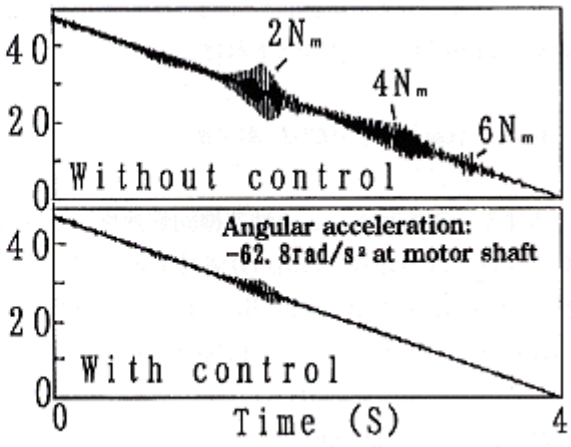

(b) Reducing the motor speed

Fig.7 Configuration of the geared motor system with the variable self-compensating control loop

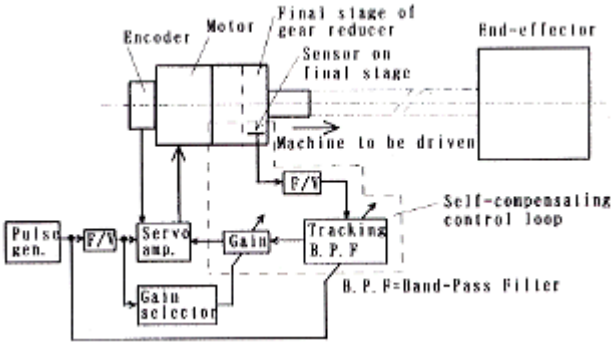

Fig.8 Suppression effects under no-loading

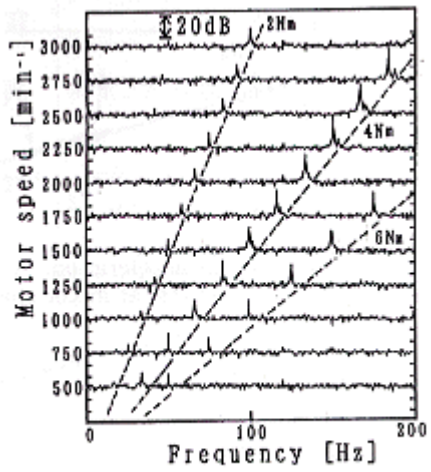

(a) Without control

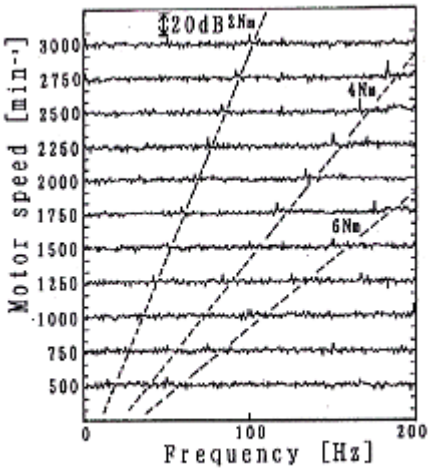

(b) With control

Fig.9 Configuration of the experimental set-up with loading inertia

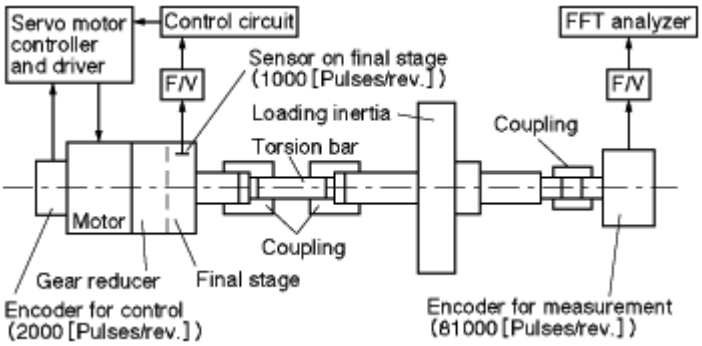

Fig.10 Suppression effects on the rotational speed variations in the case with loading inertia

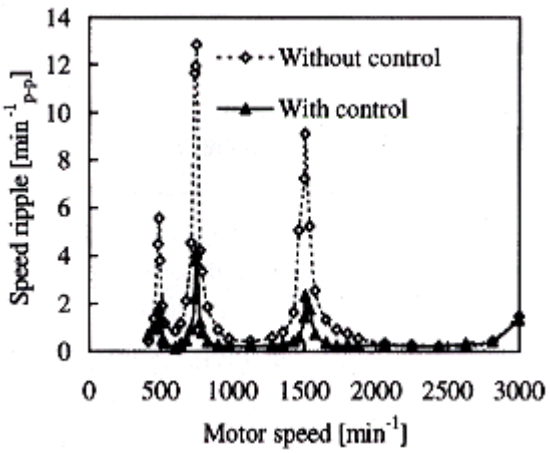

Fig. 11 Suppression effects when passing through resonance (experiment)

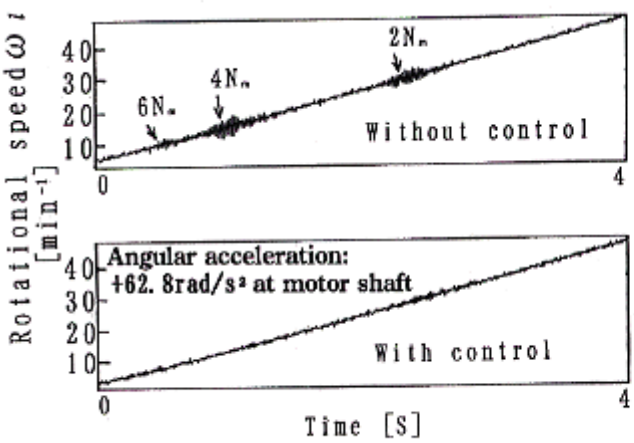

(a) Increasing the motor speed

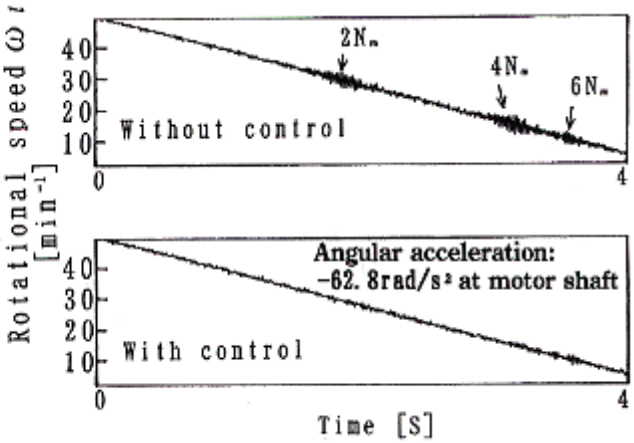

(b) Decreasing the motor speed